8-2021

# Using Single-Molecule DNA Flow-Stretching Experiments to See the Effects of Temperature and Viscosity

Fatema Tuz Zohra
*The University of Texas Rio Grande Valley*

# USING SINGLE-MOLECULE DNA FLOW-STRETCHING EXPERIMENTS TO SEE THE EFFECTS OF TEMPERATURE AND VISCOSITY

A Thesis

by

Fatema Tuz Zohra

Submitted to the Graduate College of
The University of Texas Rio Grande Valley
In partial fulfillment of the requirements for the degree of

MASTER OF SCIENCE IN ENGINEERING

August 2021

Major Subject: Mechanical Engineering

# USING SINGLE-MOLECULE DNA FLOW-STRETCHING EXPERIMENTS TO SEE THE EFFECTS OF TEMPERATURE AND VISCOSITY

A Thesis
by
Fatema Tuz Zohra

COMMITTEE MEMBERS

Dr. HyeongJun Kim
Co-Chair of Committee

Dr. Horacio Vasquez
Co-Chair of Committee

Dr. Yingchen Yang
Committee Member

August 2021

# ABSTRACT

Fatema Tuz Zohra, Using Single-molecule DNA flow-stretching experiments to see the effects of temperature and viscosity. Master of Science in Engineering (MSE), August, 2021, 47 pp., 20 figures, 48 references.

Deoxyribonucleic acid (DNA) is a highly charged long and semi-flexible polymer of which length is much longer than cell dimensions at least by 1,000-folds. A long linear DNA turns into a crumpled structure to fit into a tiny cell volume by the process known as DNA compaction. In nature, DNA fits into the volume of the cell using DNA compaction by packaging genome material. Various types of protein are involved in DNA compaction. To experiment with various proteins as DNA compaction agents, DNA needs to be stretched out. In our thesis, the effect of temperature and buffer viscosity on DNA stretching and fluctuation was observed using steady-state laminar flow. From experimental data, a slight increase in length, with the increase of temperature and viscosity was found out. The total change of the stretched length of DNAs was almost 0.7μm - 0.8 μm for 0 %PEG in EBB buffer to 5% PEG in EBB buffer solution in our experiment. The total increase of length from 4 ºC to 30 ºC was almost 0.5 μm which is almost linear. It was observed that temperature changes did not lead to a noticeable change in the fluctuation of DNA, but when buffer viscosity was increased, the fluctuation of DNA decreased. The average fluctuation of DNAs for 3% PEG and 5% PEG are 15% and 28% lower than the fluctuations of DNAs for EBB buffer. Thus, it can be concluded that DNA length and fluctuation are a function of viscosity.

# DEDICATION

Thanks to the almighty. My journey at UTRGV for the Master's studies would not have been possible without the love and support of my Supervisor Dr. HyeongJun Kim, Dr. Horacio Vasquez, Dr. Yingchen Yang, my parents, my sister, my husband, and my friends. I dedicate this work to my baby girl Amira Fatema Abdullah who was always with me.

ACKNOWLEDGMENT

First of all, I would like to acknowledge my supervisor, Dr. HyeongJun Kim for his support and guidance. His continuous mentorship along with his excellent vision and expertise. I also want to express my gratitude towards my parents who always help to achieve my dream. Their support helps me to stand in the place I am now.I want to give my gratitude to my husband who always supports me in my good time and bad time. I would also like to thank my baby girl Amira Fatema Abdullah for becoming such a sweet little girl and understand and support mummy at this young age.

TABLE OF CONTENTS

Page

LIST OF FIGURES

Page

# CHAPTER I

## INTRODUCTION

Deoxyribonucleic acid (DNA) is a long highly charged, and semi-flexible polymer, which stores genetic information in all cells. The total length of DNA in a human cell is 2 m [1], whereas the nucleus of each human cell is only about 10 μm in diameter [2]. Therefore, long and linear DNA needs to be compacted to fit into this tiny volume. The process in which a long linear DNA turns into a crumpled structure to fit into a tiny cell is known as DNA compaction [3]. It occurs in a highly dynamic and organized fashion. Multiple elements such as DNA-binding proteins are involved in this process. One of the important elements is known to be DNA-binding proteins [3]. DNA-binding proteins compact DNA by bending, wrapping, or bridging to package it within the cellular volume [3]. DNA compaction is important for maintaining and regulating genetic information. Gene regulation is one of the most important applications for DNA compaction. Besides, DNA compaction is important for DNA manipulation and fabrication of nanostructure [4]. Reversible DNA compaction can be a protector of DNA from biochemical, mechanical, and chemical stress [4]. Regulation and Packaging of gene expression are the major roles of DNA compaction [4]. Due to the importance of DNA compaction in various aspects of genome regulation and maintenance, a growing number of intensive studies on DNA compaction have been done (Figure1). Supercoiling and DNA compaction play important role in gene transcription. The effect of DNA compaction on transcription was first studied in 1987, by Baeza *et al*.[5]. They have reported the enhancement

in gene transcription because of DNA compaction [5]. However, the result of this experiment could not be verified due to the lack of evidence. Recently, Tusmoto *et al.*(2003) showed a sharp inhabitation in transcription activity due to DNA compaction. polyethylene glycol (PEG) and spermine were used as compacting agents in their experiments [6]. Another study demonstrated DNA compaction as an on/off switching of transcription [6], [7]. They used an elegant fluorescence resonance energy transfer (FRET) assay for detecting a single-molecule of mRNAs. The mRNAs were in water-oil-based microdroplets which were coated with a phospholipid membrane. [4], [7]. Photocontrol of DNA compaction allows controlling gene expression on both transcription and translation levels [4]. DNA compaction and reversible DNA compaction can be a protector of DNA from biochemical, mechanical, and chemical stress [4]. Another use of DNA is as a nanostructural template [8]. DNA template offers a broad range of nanostructure sizes and shapes. Nanomaterial deposition with DNA templates can be applied to a wide range of materials like Ag, Pd, Cu, Ni, Co, Au, Pt, oxides, and semiconductors [4], [9]–[12]. DNA as a template for nanostructure can open an immense possibility for its size and variety.

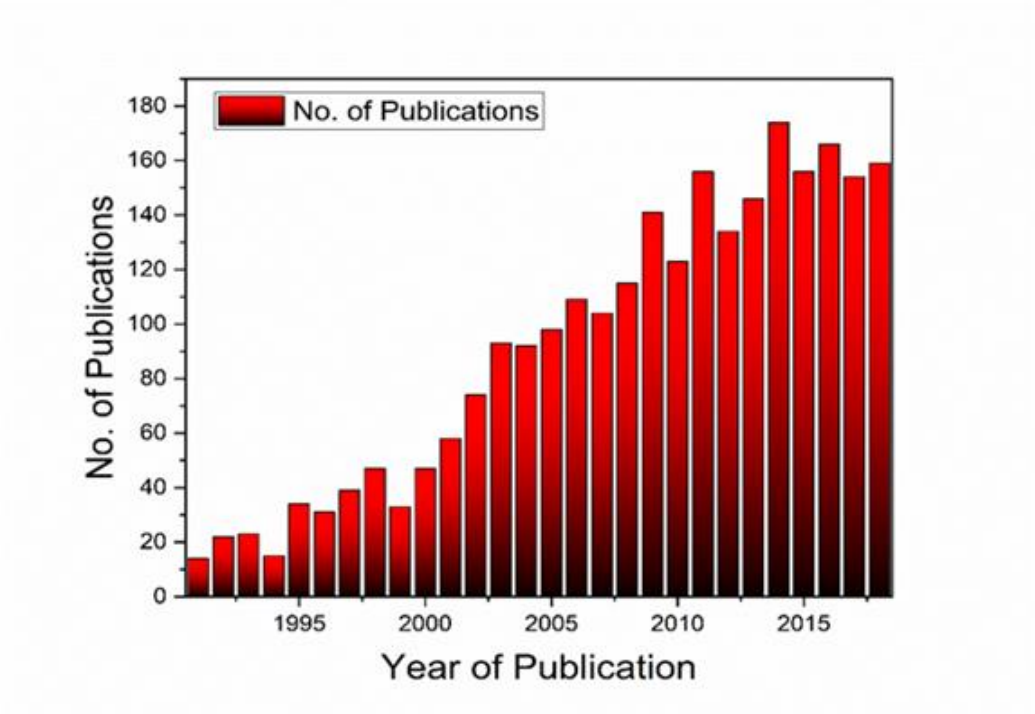


Figure 1: The trend of the number of publications on DNA compaction over the years. (Data received from Web of Science)

In DNA compaction experiments, DNA is stretched out using different force fields to see the effect of various compacting agents. Single DNA molecules can be stretched and manipulated by flow, electric, magnetic, and optical fields [13]. Flow fields are probably the most convenient because it does not need complex tools such as optical or magnetic tweezers or high-frequency electric fields like the others [12], [13]. Water-based solutions are generally used to study DNA compaction. One of the reasons behind this is that DNA adopts an elongated coil confirmation due to the strong repulsion between negatively charged phosphate groups [14]. Thus, proteins can recognize binding sites with variable sequence lengths. Upon addition of appropriate compaction agents, DNA undergoes a strong compaction process. Stretching out of DNA is a crucial part of DNA compaction experiments, as proteins can recognize binding sites with variable sequence lengths. In our experiment, the laminar flow flowed through a

microfluidic flow cell where DNAs are tethered to the surface at one end. The other end was labeled with a quantum dot that emits fluorescence signal upon laser excitation to see the conformational changes of flow stretched DNA at different temperatures and viscosity. The range of 'microfluidic' focuses on the ability to manipulate fluids in the 5–500 μm range [15], [16]. Microfluidic flow cells contain single or multiple flow channels where flows are driven through. Recent developments in this field, make it a powerful tool to study the micrometer scales, such as DNA helicases, DNA packaging motors, dsDNA (double-stranded DNA) translocases, nucleases, DNA polymerases, RNA polymerases, RNA helicases, and DNA and RNA dynamics [17]–[20]. Microfluidics is equally important in the field of engineering, medical and biological science. In particular, microchannels are frequently used to study the mechanical properties of these substances.

Single-molecule biophysics provides powerful methodologies to study biomolecules. In conventional ensemble experiments, a large number of molecules is observed at the same time[21]. The results are then averaged out to determine their properties. This can be correct or may not be correct because biomolecules generally have heterogeneity. So, the result from conventional ensemble techniques may need to be corrected sometimes. Single-molecule needs to be studied at a time to determine this heterogeneity [4], [22]. Single-molecule experiments study one molecule at a time which makes single-molecule biophysics a powerful tool to study heterogeneity. Sometimes, surprising and noble information is achieved through these techniques which provides an access to valuable molecular information [22]. The single-molecule method is a strong tool for studying complex chemical and biological systems. Firstly, these techniques measure biological molecules one at a time. In contrast, for conventional ensemble experiments, they interrogate a large number of molecules at a time and infer their

properties by averaging the output results. The single-molecule technique can measure molecular properties more directly. For example, single-molecule biophysics can directly observe multiple distributions of folding states of protein when ensemble experiments can only give indirect results [23]. This technique can be used to measure dynamic systems with rare species or states under equilibrium conditions. This technique is vital for the elements of dynamic systems that are difficult to synchronize. For example, the movement of DNA enzymes along their track is very complicated and stochastic. As a result, it is difficult to synchronize at a significant distance during this movement. Single-molecule methods can be utilized to study these modalities [24]. The single-molecular technique can also be applied to directly measure the kinetic rate constant and connectivity of different systems and different states [28]. Additionally, molecular structure, their functional responses, as well as molecular force, can be measured directly with single-molecule manipulation [28]. At large concentrations, some biological molecules show aggregation behaviors. The single-molecular technique allows the study of these biological molecules as well. The properties of the monomeric species can also be monitored using single-molecular technique at low concentration and equilibrium conditions.[25], [26], and single-molecule techniques can study their original concentrations. Single-molecule biophysics developed only about 30 years ago. In only less than 30 years of its lifetime, its application in different fields is growing tremendously [21]. Scanning tunneling microscopy(STM) [27] and atomic force microscopy (AFM) [28] are used to image individual DNA molecules in water. The first single fluorophore was detected at liquid helium temperature in 1990 [29]. Later the experiment extended to room temperature which in turn opened the possibilities of biological and chemical implementation [21]. During the mid-1990s, single-molecule fluorescence and manipulation techniques were used to study more complicated and sophisticated biological

systems. The discovery of DNA melting and overstretching transition was propagated due to the application of optical tweezers and glass fibers during DNA stretching [30]. During the movement of myosin, individual Adenosine Triphosphate (ATP) turnovers can be observed directly using fluorescence imaging [31].

Broadly speaking, the single-molecule technique can be defined into two categories; Fluorescence imaging and spectroscopy and force-based manipulation and detection. Some examples of force-based manipulation and detection include optical traps and magnetic tweezers. Optical traps use tightly focused lasers to apply force and small movement to molecules. There are single beam and dual-beam optical tweezers with nanometer resolution. Magnetic traps can apply torque and thus control the supercoiling nature of DNA [4], [21], [22].

Fluorescence imaging and spectroscopy can be divided into two areas; *in vitro* and *in vivo* [21]. When experiments are performed in live cells it is called *in vivo* [21]. On the other hand, when experiments are performed inside tubes it is called *in vitro*. Experiments in *in vivo* have a number of challenges. But it has become possible by using fluorescence-labeled quantum dots. The fluorophore is a chemical that emits fluorescence upon excitation. Single-molecule fluorescence detection is achieved when fluorophores are repeatedly excited and the emitted fluorescence photon is then detected and analyzed. The fluorescence emitted by the fluorophore is limited [21]. As a result, the single-molecule technique needs bright fluorophores and a high efficient and low-background photon detector [21], [23]. High-efficiency optics are required for the collection of a large number of photons [29]. Objectives with a high numerical apertures (numerical aperture N.A: 1.2 or higher) are used to collect a large number of photons. Also, single-molecule techniques need a high-sensitivity photon detector (CCD or EMCCD camera). This helps to minimize the effects of scattering and fluorescence from buffers and impurities. To

minimize background photon, total internal reflection (TIR) and confocal are mostly used to study single-molecule fluorescence [21], [23]. Total internal reflection fluorescence microscopy (TIRFM, Figure 2b,c) was used in our experiment. TIRFM creates a very thin evanescent field (approx. 100–200 nm thick) that is very close to the interference which in turn avoids background fluorescence from the rest of the samples.

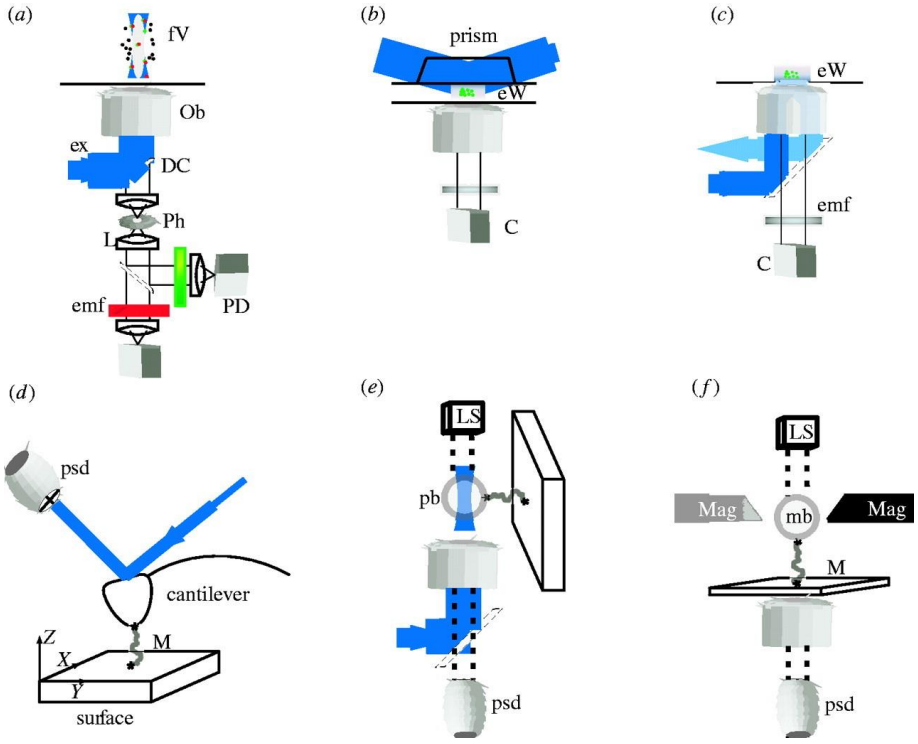


Figure 2: Examples of six single-molecule instrumentation (a) Confocal geometry and dual-color detection; fV is focal volume, Ob is objective, ex is excitation with laser, DC is a dichroic mirror, Ph is pinhole, PD is point detector, emf is emission filter. (b) Prism-type TIRFM. (c) Through-objective TIRFM; eW is an evanescent wave, C is an area detector or camera. (d) AFM; psd is the position-sensor detector, M is the molecule. (e) Optical tweezer; LS is the light source, pb is polystyrene bead. (f) Magnetic tweezer; Magis magnet, mb is the magnetic bead. The figure is taken from Reference [22]

In TIR fluorescence microscopy, an incident beam of light undergoes TIR at the surface between two materials of high and low refractive indices. A narrow evanescent field is formed in the lower refractive index material. The field is approximately 100-200nm thick.[45]. This mechanism is the physical basis for TIRFM. In TIRFM, only the molecules near the coverslip surface are illuminated. Using this techniques molecules within 100 nm can be visualized. [45]

Some of the examples of fluorescence imaging and spectroscopy include FRET, FIONA, fluorescence correlation spectroscopy, and so on [21], [32].

FIONA stands for fluorescence imaging with one-nanometer accuracy that has been used to localize a single dye or group of single dyes with approximately 1 nm accuracy [21]. This accuracy is achieved by using TIRF, deoxygenation agents, high quantum field, and low noise detector [32]. In the FIONA technique, fluorophores are placed on a coverslip and excited with some method, the most successful one is utilizing total internal reflection fluorescence microscopy (TIRFM). The reason behind this is that TIRF requires a very small fluorophore volume and background fluorophores are also very low [21]. A charged-coupled camera (CCD) or an electronic multiplication charged-couple camera (EMCCD) collects fluorescence and the intensity is plotted as a function of x and y [21]. But one of the major challenges of this process is light diffraction. A small size appears to be a big object because of light diffraction. In our experiment, the fluorescence-labeled quantum was 20 nm in size. However, it appeared 200 nm because of light diffraction [Figure 3].

According to the FIONA technique when the fluorescence is plotted as a function x and y, the point-spread function is fitted by two-dimensional Gaussian functions [32]. The main objective is to determine the mean value of the distribution and its uncertainty which is positional accuracy or the standard error of the mean [33]. Thompson *et.al* showed that

approximate localization is equal to the width of the point spread function (PSF) divided by the square root of the total number of photons when sufficiently enough number of photons were collected [21]. But some variables like background noise must also be considered.

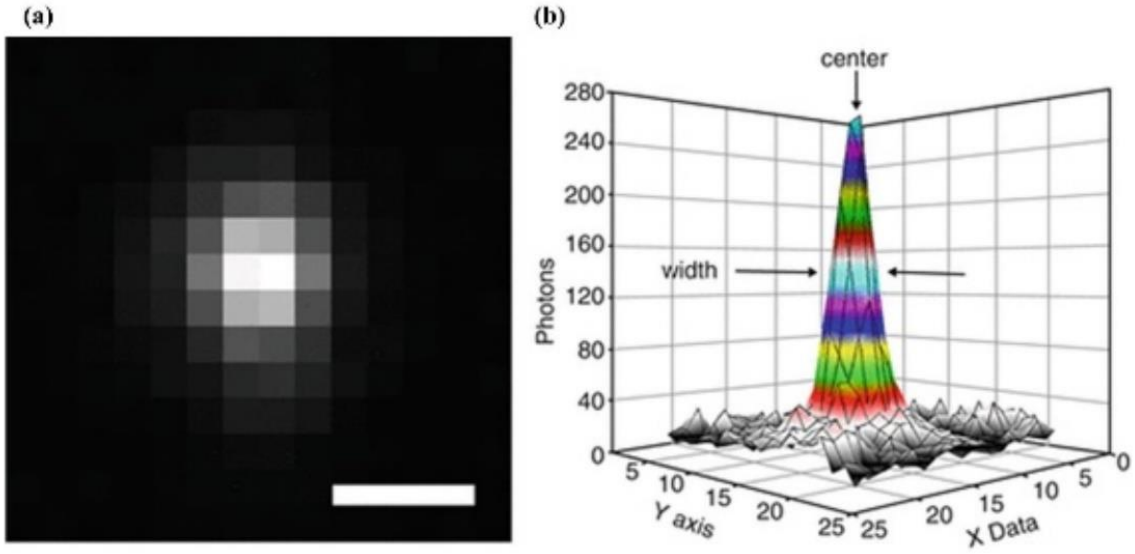


Figure 3: An EMCCD image and its point spread function. The actual size of the flurophores is 20nm. But because of light deffraction, the appered size is much bigger than the actual size. Scale bar denotes 400nm. (1 pixel = 107 nm) [33]

The standard error of the mean, σμ can be described by the following equation.

$$\sigma_{\mu i}=\sqrt{\left(\frac{S_i^2}{N}+\frac{\frac{a^2}{12}}{N}+\frac{8\pi S_i^2 b^2}{a^2 N^2}\right)}$$

Where,

S= Standard deviation.

N= number of photons.

a= Pixel size of CCD or ECCD camera.

b= standard deviation of background.

The first term ($\frac{S_i^2}{N}$) is the photon noise, the second term is the effect of the photon size of the pixel of the detector and 3rd term is the effect of the background. The recommended pixel size ranges from 80 to 120 nm [32], [36].

When a large number of photons are collected, the second and third terms are negligible so the standard error of the mean, σμ is

$$\sigma\mu=\frac{S_i}{\sqrt{N}}$$

In the experiments employed for this thesis work, fluorescence-labeled quantum dots were attached at one end of the DNA, and an EMCCD camera and a TIRF microscope were used. One dimensional Gaussian fit was used in the y-axis. Custom-written MATLAB codes were used for data analysis.

Another challenge about intracellular organelles which we need to overcome is that, in addition to having water molecules, ions, metabolites, and other small solutes—typically they contain other macromolecules such as proteins, nucleic acids, ribosomes, and lipids which is between 200 and 400 g/L of mass per unit volume [34]. The complex environment can happen because the crowding and confinement of these biological compounds may impact *in vivo*

biomolecular function. Reduction of diffusivity is one of the most common consequences. Crowder molecules also have an effect on macromolecular folding and stability and internal dynamics [34]. The effect of this crowded cellular environment is very significant in the activity of biomolecules. High viscosity fluid was used in this experiment to stretch DNAs to study the effect of a crowded cellular environment. Our study proved that the stretching and fluctuation of DNA are a function of viscosity. One of the consequences of the viscosity of the fluid is viscous drag Fv. Viscous drag force is basically a resistance force that is employed on a dynamic object. When laminar flow flows around a sphere in a fluid flow, drag force Fv is proportional to the viscosity of the fluid η, and speed of the flow v, and the characteristic size of the object L. So, higher drag force is expected for higher viscosity of the fluid and larger size of the object. Because of Fv, DNA stretching increases with the increasing viscosity of the liquid [37], [38].

A central property of DNA is helicity. The helicity of DNA is ∼10.5 bp/turn [39]. The helical twist depends on temperature. With the increase of temperature, DNA twist unwinds Initially, it was estimated that the rate of the change of the helical twist Tw(T) varied from −4 to −5º/(ºC·kbp) by measuring circular plasmids and electrophoretic mobility [39]. Later, for thermophilic temperature which is close to DNA melting, a linear dependency on temperature was observed up to 80 ˚ C with a coefficient of 10.5º/(ºC·kbp) using electrophoretic mobility [39]. Strick *et al.* (1998) used a magnetic tweezer experiment to determine the dependence of DNA twist on temperature [39]. The helix unwind was found to be 30% larger (−13.4º/ºC·kbp) than the previous study. Kriegel F. *et al.* (2018) [39] have experimented on the effect of temperature on DNA helix at different temperature. They used a unique and custom-built temperature-controlled magnetic trap to study the changes of DNA twist with respect to temperature. They observed that with the increase of temperature DNA unwinds, even for the temperature which is much lower

than the melting temperature. They found that DNA unwinds with a rate of $T_w(T) = (-11.1 \pm 0.3)^\circ/(^\circ C \cdot kbp)$ [39]. The increase of the temperature diminishes the stabilize state of the DNA helix. So, this theory predicted that with the increase of temperature, the overstretching force will decrease. DNA overwinds, under small force (<30 pN) [47]. DNA can be extended by 0.5nm/turn due to overwinding. [47]. One of the explanations for this phenomenon is the reduction of the inner core radius [47]. The overstretching force of DNA is a function temperature, and with the increase of temperature, the overstretching force decreases [35].

Jiang, H. R., & Sano, M. (2003) have found that if temperature gradients are applied to DNA, they create internal tension on the DNA, and DNA stretches out [40]. They measured conformations of one end tethered and two ends tethered DNA in different temperature gradients, up to 3 K⁄μm. They have observed that the length of DNA increases with the increase of temperature gradient. In this experiment, the concept of single-molecule biophysics is used to see the conformational changes of flow stretched DNA at different temperatures and with different viscosity [40].

In this thesis paper, the effects of temperature and viscosity on flow-stretched DNA have been studied. The changes in fluctuation with the change of temperature and viscosity have also been investigated. In our experiment, the temperature of the buffer solution was increased from 4 ºC to 30 ºC to study the effect of the temperature on DNA stretching. For the viscosity experiment, three different solutions with three different viscosity were applied and the results were compared to see the effect of viscosity on flow stretched DNA.

In the following chapter, materials, and methods, the results of the experiment, summary of the experiment are discussed in detail.

# CHAPTER II

## EXPERIMENTAL SETUP

In our experiments, single-molecule biophysics visualization was used to investigate the effects of different buffer temperatures and viscosities on the lengths of flow-stretched DNAs. One end of the bacteriophage lambda DNA was tethered to the microfluidic flow cell surface and the other end was labeled with a fluorescent quantum dot (Qdot). The fluorescence signal from the Qdot was tracked using Total Internal Reflection Fluorescence (TIRF) microscopy. A heat-block (figure 7) was used to control buffer temperatures. Firstly, coverslip, quartz top, and double-sided tape were used to make a two-channel microfluidic flow cell (see Figure 4). The surface of the coverslip (also called cover glass) was passivated with mPEG (Methoxy polyethylene glycol) (96 %) and biotin-PEG (4 %) to minimize nonspecific DNA bindings [48]. The biotin-PEG allows one end of the biotinylated lambda DNA to be tethered to the surface via neutravidin-biotin interactions. Polyethylene tubes with a dimension of PE number: 60, wall thickness: 0.009”, were used as an inlet and an outlet of the flowcell [48]. A quartz top was used to accommodate these four holes. The dimension of this quartz top is 20 mm x 25 mm x 1 mm [48]. Cover glass and quartz top was attached using a double-sided tape. The thickness of the tap was 0.12 mm [48]. Flow channel layout was used to create the flow channel which was drawn on the tape and then cut off [48]. Thus, the thickness of the tape was the thickness of the flow channel [48]. The width of each channel was 1.8 mm [48]. For our experiments with different buffer viscosity, the length of the inlet tubing was 13 cm and for the experiments with different

temperatures, the inlet tubing was 30 cm long. In both cases, the length of outlet tubing was 1.5 to 2 cm.

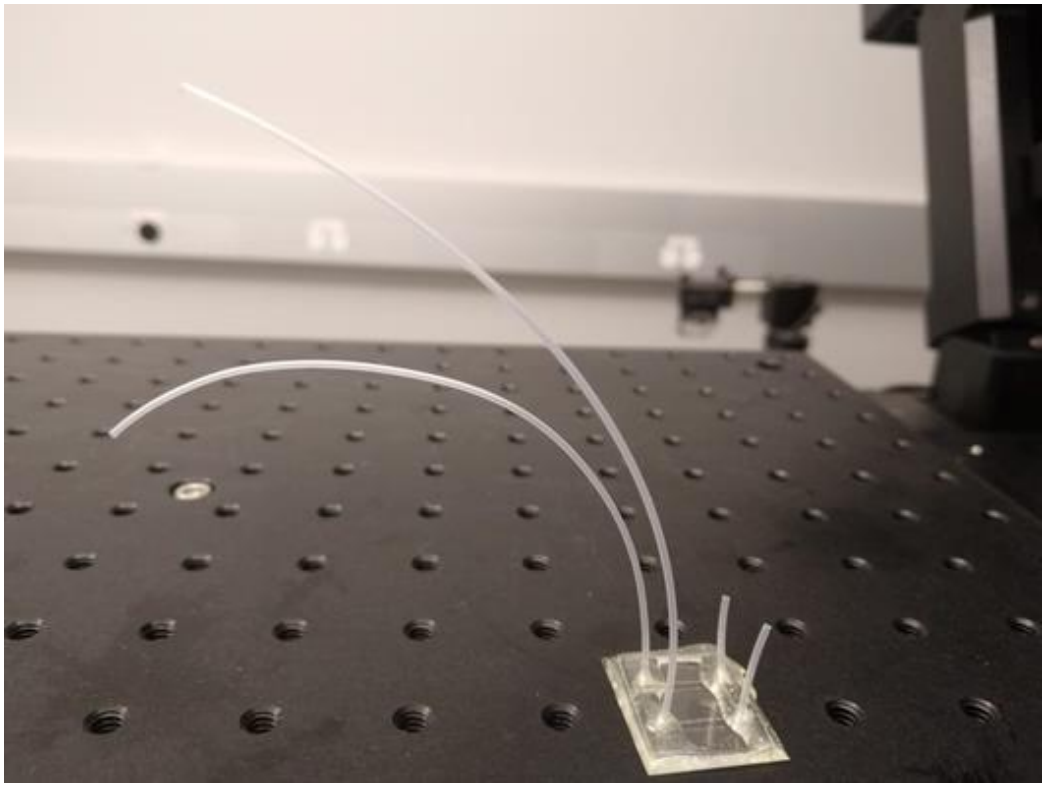

Figure 4: Two-channel microfluidic flow cell.

Bacteriophage lambda DNA used its complementary single-strand 5' overhangs to label DNA with biotin- and digoxigenin- oligos [48]. Bacteriophage lambda DNA was labeled with biotin at one end and digoxigenin at the other end (Figure 5) [48]. The biotinylated end was tethered to the surface of the PEGylated cover glass through biotin-neutravidin (or biotin-streptavidin) interaction [48]. The end with digoxigenin was used in labeling a fluorescent quantum dot.


Figure 5: Figure shows how one end of the DNA is labeled with biotin and the Other end is labeled with digoxigenin which was attached to the fluorescence-labeled quantum dot. (Figure: Courtesy of Dr. HyeongJun Kim)

Next, 2.7 µL BL1-Dig2-Lambda-DNA with 0.3 µL of 32x-diluted (~30 nM) anti-Dig antibody-conjugated Qdot 605 was incubated in the presence of 16.7 µL EBB buffer for 5 minutes. The composition of EBB buffer is 10 mM Tris pH 8.0, 150 mM NaCl, 10 mM $MgCl_2$. Using a syringe, add 57 µL of 0.25 mg/mL of neutravidin to the flow channel through the inlet tubing. Incubate for 5 minutes. After 5 minutes, 180 µL EBB buffer was inserted into the tubing using pipette tips which helped to reduce bubbles formation when connected to the syringe pump. Figure 6 shows the experimental setup. A syringe pump was used to pump the solution with a controlled flow rate. The outlet of the flow cell is connected to the syringe of the syringe pump and the inlet was connected to the solution.

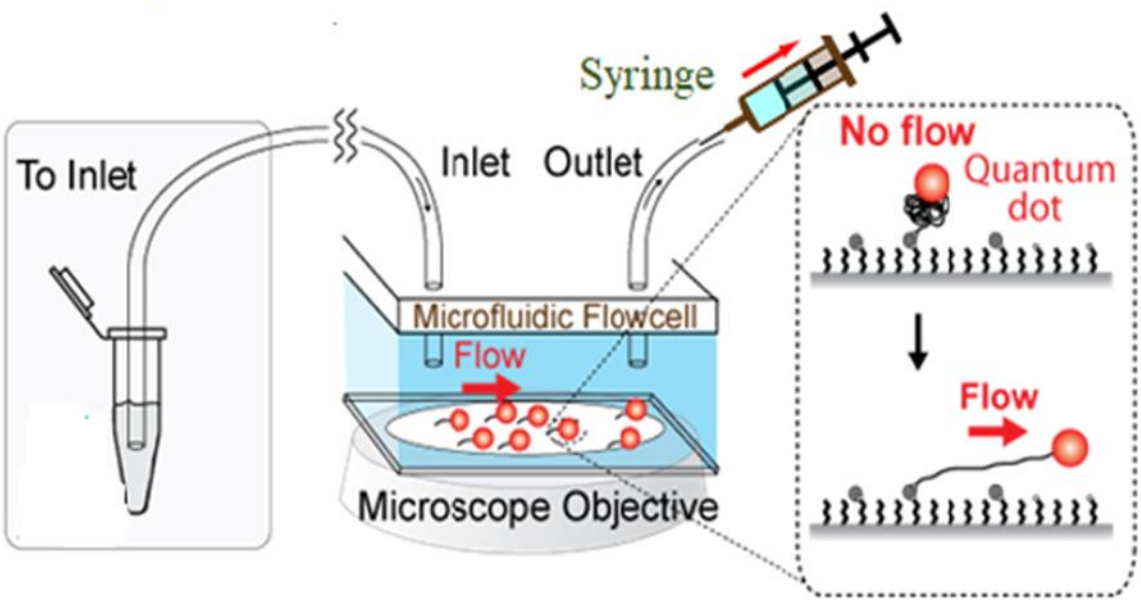


Figure 6: Experiment setup.

The syringe pump pulled the solution through the flow channel by pulling syringe plunger [48]. We added 350 µl EBB+BSA (bovine serum albumin) buffer with 10 µl incubated DNA–Qdot solution and flowed this solution into the flow channel with a flow rate of 30 µl/min. The biotinylated end was tethered to the surface of the PEGylated coverglass by biotin-neutravidin (or biotin-streptavidin) interaction.

For the DNA flow-stretching experiment with different buffer viscosity, after flowing the DNA-Qdot buffer solution, we flowed EBB buffer (without PEG) through the flow channel first followed by EBB buffer supplemented with 3% PEG or 5% PEG. EMCCD camera captured this experiment and exposure time was 200 milliseconds. We took around 1500-2000 frames. For the first 100-150 frames, there was no flow. The position of the Qdot in this region is the tethered point or unstretched DNA length. DNA stretched length was calculated alone at this point. As, in the viscosity experiment, EBB buffer flowed first before 3% or 5% PEG solution; when data were collected for 3% or 5% PEG, the first 300-400 frames contain only the effect of EBB buffer

on DNA stretching.  An exposure rate means the photons will be captured every 200 msec. Different experiments were conducted for 3% PEG in buffer solution and 5% PEG in EBB buffer. In DNA flow-stretching experiments, for investigating effects of different temperatures, after flowing the DNA-Qdot buffer solution, EBB buffer was used. The temperature of the buffer solution was manipulated using a heat block (Figure 7). In our experiment temperature of the buffer was increased and flowed through the flow cell. Thus, all the DNAs experienced the same temperature.


Figure 7: Heat block

Figure 8 shows the experimental setup of our experiment. In this picture, we can see the air spring, syringe pump, and flow cell. In the figure, the inlet tube of the flow cell is dipped into the buffer solution. The driving force for flow speed is the syringe pump which is attached to the air spring. Air spring is attached to the outlet tubing. The speed we got from the syringe pump was not smooth rather it was jerky motion. The air spring made flow smooth. The quantum dot was excited with 532 nm laser light, and it emitted fluorescence. The fluorescence, which was

emitted by quantum dots, was detected by the EMCCD camera. TIRF microscope was used in this experiment, so the background noise is negligible.

The data were analyzed using MATLAB. To analyze the data, ImageJ software was also used. We opened the TIFF file of the movie using ImageJ software. Then, regions of interest (ROI) for both Cy3 and quantum dot channels were selected. The list of ROI (information of the selected area) is imported to custom-written MATLAB codes that perform Gaussian fitting on the signal and determine the positions of the quantum dots over time.

For data analysis, one-dimensional Gaussian fitting was used to analyze the data. So, instead of analyzing the position of quantum dots in both x-y directions, the position of Qdots was only analyzed in the y-direction.

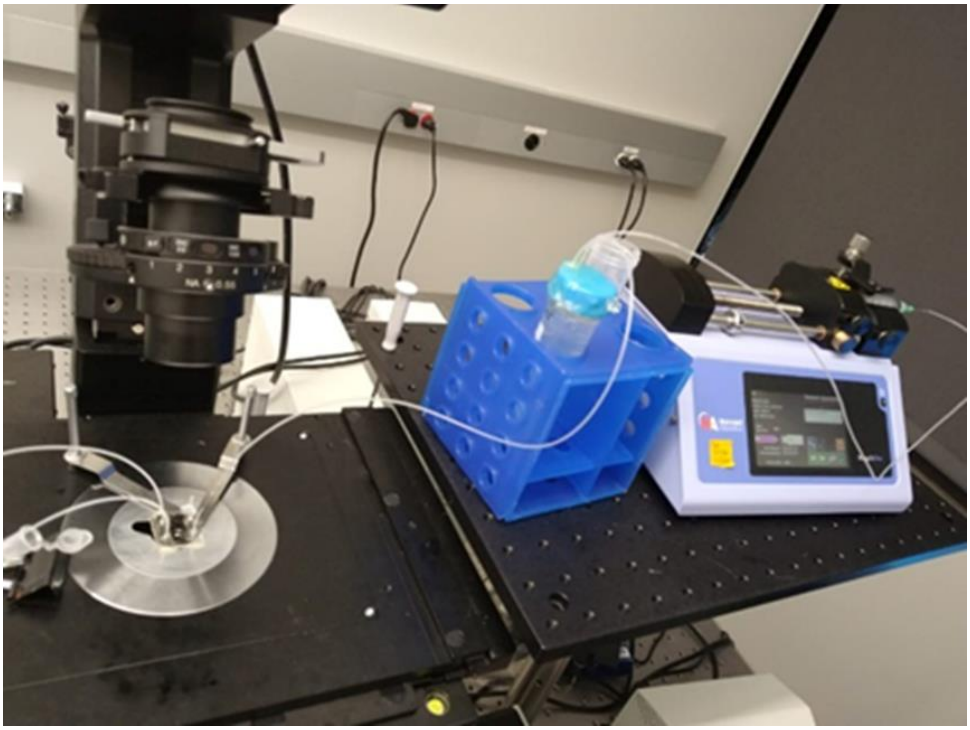

Figure 8: Experimental setup ii.

In the next chapter, the experimental result which we obtained by using the experimental setup discussed in this chapter, will be discussed. Also, the pros and cons of this experiment and future development will be discussed in the following chapter.

# CHAPTER III

## RESULT AND DISCUSSION

If DNA is removed from an organism, contacts with proteins, and is placed in water, at moderate salt concentrations, DNA behaves as a flexible, self-avoiding polymer at long length scales. This behavior is statistically identical to those expected for any linear chain in a good solvent [41]. In other words, in a water-based solution, DNA adopts an elongated coil conformation. Stretching DNA in several investigations has shown that DNA exhibits unusual elastic behavior [42]. So, if a DNA molecule is subjected to external or internal stress, DNA stretches out. However, overstretching transition happens when DNA stretched out beyond its B-form contour length overstretching transition. This force is called overstretching transition force. When DNA stretched more than 1.7 times of its B-contour length, the force increased rapidly. The overstretching force for DNA double helix is about 65 pN [43] [43]. It was found that both overstretching transition and DNA melting are the functions of temperature [35][43]. DNA melting defines as the dissociation of DNA double helix into single-stranded DNA. DNA melting point depends on both heat and force. DNA melting temperature depends on the hydrogen bonds in DNA molecules. In the experiments performed for this thesis work, laminar flow is applied to the DNA to exert force on DNA. The force, which is exerted on the DNA in our experiment, is much lower than the overstretching force (<1 pN). Thus, there is no overstretching transition of DNA in this experiment. The contour length of DNAs used in our experiments is 16 μm in length. However, the end-to-end DNA distance under our flow-condition is only up to 12 μm (Figure 9).

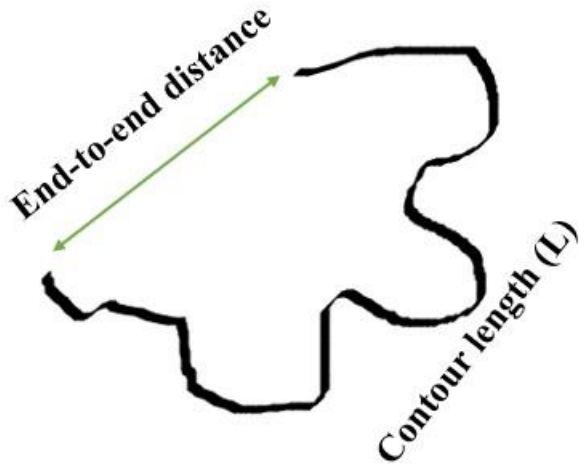


Figure 9: Contour length (L) of DNA and its end-to-end distance.

The simplest model of a linear polymer to study the elasticity and fluctuation of DNA is a string of beads that are joined by springs. Rouse's model said that each bead has the same drag and diffusion coefficients, and each bead act as a Brownian diffuser [44]. However, this model neglects the fact that each bead is under the effect of the flow field that is produced by other diffusing beads and this flow field is changing with time. This hydrodynamic interaction (HI) was included in the Zimm model and this interaction is the reason for the linear dynamics of the polymer [44]. However, the Zimm model includes hydrodynamics interaction between beads. According to him, each bead interacts with its neighborhood beads [44]. Although mathematical techniques were applied to calculate exact results for fluctuating hydrodynamics, this is not enough. To calculate the internal HIs of polymer dynamics more sophisticated mathematical techniques are needed. Because this field is still unsolved [44].

An international team (Berkley Lab) experimented on the flexible nature of DNA molecules, from the Berkeley National Laboratory under the Department of Energy's Lawrence

and they successfully captured the flexible nature of DNA. They attached gold nanoparticles to both ends of the DNA molecule. High-resolution 3-D images were captured to observe each DNA segment. Figure 10 shows the flexible structure of the DNA segments, which can be compared with jump ropes at the nanoscale.

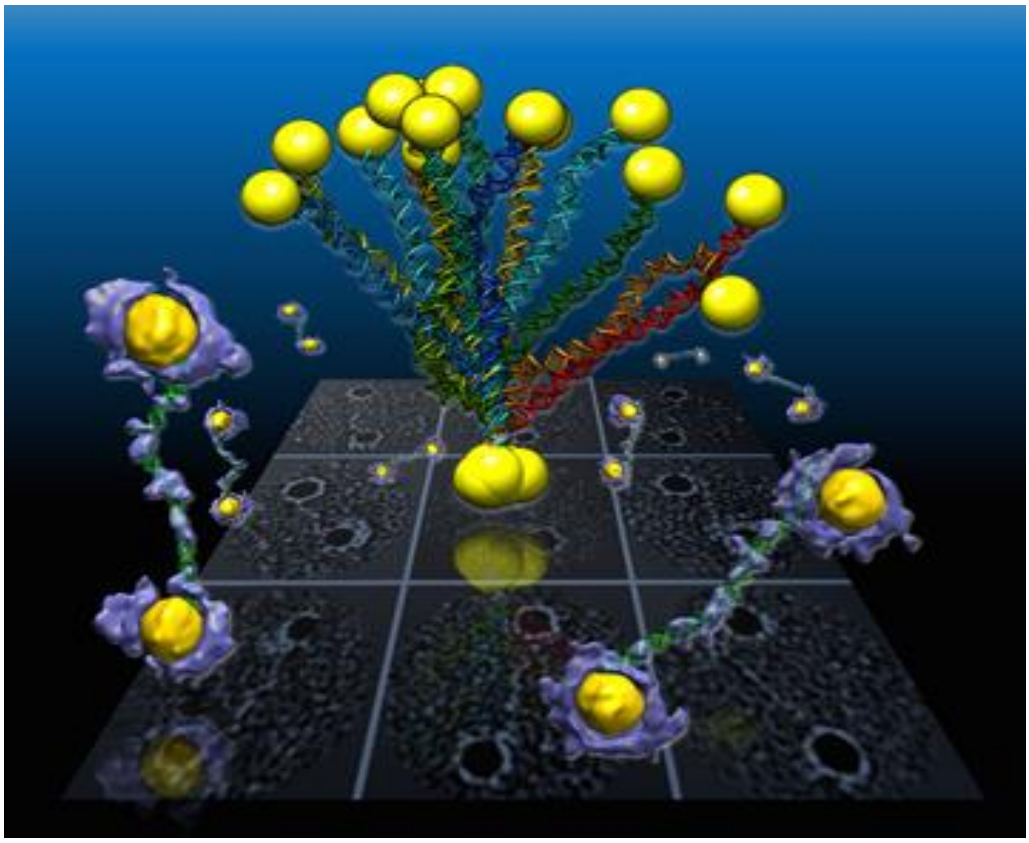

Figure 10: In this figure, the flexible nature of the double-helix DNA segments is shown. Both ends of this segment were connected to gold particles. The 3-D density maps, labeled with yellow and purple which are shown in this figure were reconstructed at Berkley lab from the induvial segment of DNA. They used individual-particle electron tomography or IPET to reconstruct these maps. (Credit: Berkeley Lab) (Revealing the Fluctuations of Flexible DNA in 3-D." https://newscenter.lbl.gov/2016/03/30/revealing-the-fluctuations-of-flexible-dna-in-3-d/ (accessed Jul. 12, 2021).

In our experiment, the fluctuation of DNAs at different temperatures and viscosity was also calculated, to see how DNAs behave at different drag forces and temperatures. To see the effect of drag force on the fluctuation of DNAs, three different buffer solution with three different viscosity was used at room temperature. The temperature of the buffer solution was increased from 4ºC to 30ºC to see the effect of temperature on the fluctuation of DNA. To calculate the fluctuation, the standard deviation of the stretched length of DNAs for different conditions was calculated.

### 3.1 Effect of viscosity in flow stretched DNA

As we discussed earlier, cellular environment is very crowded which may impact biomolecular function *in vivo*. But *in vitro* experiments, this effect is often not considered. The goal of our experiment is to observe the effect of the crowded cellular environment on flow stretched DNAs. We have investigated the effect of viscosity in flow-stretched DNA by utilizing polyethylene glycol (PEG) as a crowding reagent. At constant temperature, four different buffer solutions of four different viscosities were used in our experiment: EBB (10 mM Tris pH 8.0, 150 mM NaCl, 10 mM MgCl2), the ones supplemented with 3% (w/V) PEG, 5% (w/V) PEG, and 10% (w/V) PEG. But DNAs got stuck on the surface of the cover glass when 10% PEG (w/V) was used. Brookfield digital rheometer MODEL DV-III+ was used to measure the viscosity of each solution. We have performed three different measurements for each sample and each condition. We have increased revolutions per minute (rpm) from 20 to 100. Figure 11 shows the measured viscosity of four different buffer solutions with different rpm of the spindle of Brookfield digital rheometer MODEL DV-III+.

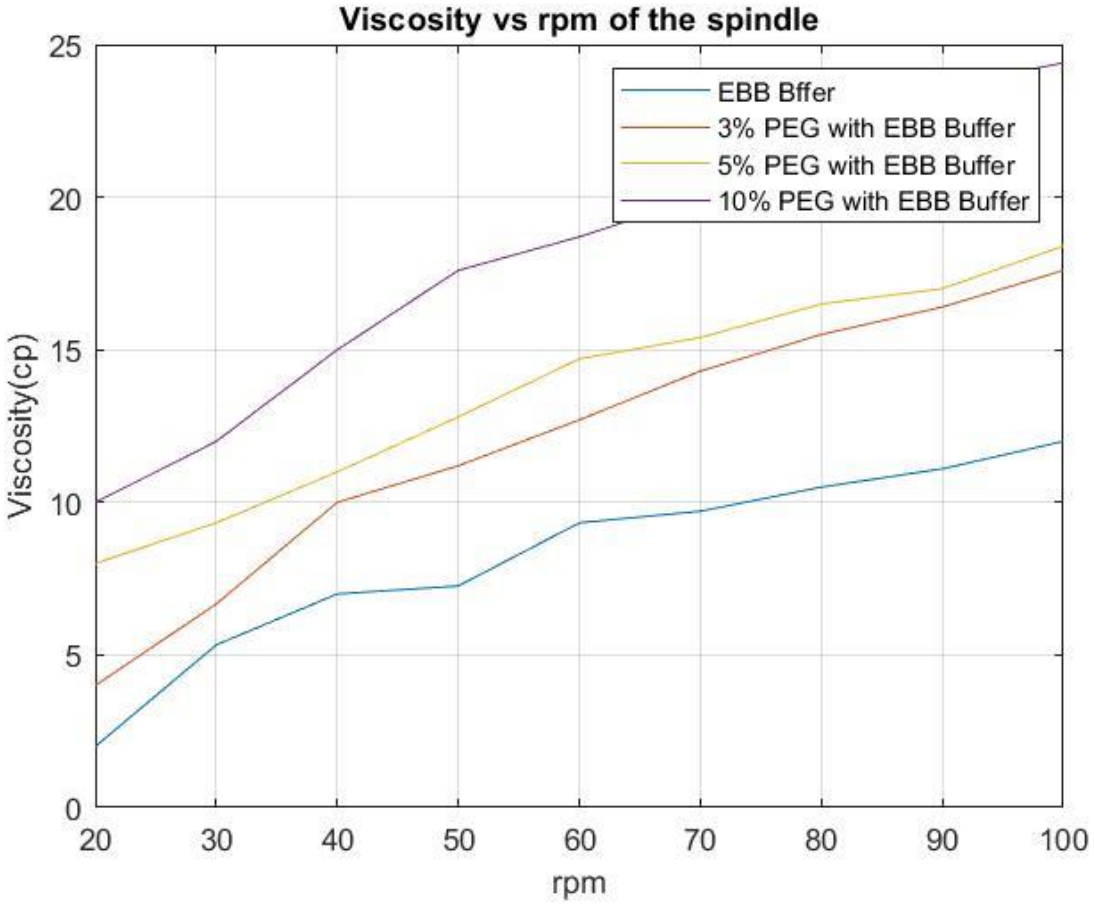


Figure 11: Viscosity of different solutions with the spindle rpm at 22 ºC. rpm of the spindle was changed from 20 to 100. The viscosity of the solutions depends on applied stress. The viscosity of 10% PEG with EBB Buffer solution is higher than other solutions. The unit of the viscosity of the graph is cp which stands for centipoise which is equal to mPa´s.

Figure 11 shows the measured viscosity for different rpm of the spindle. It was observed that with the increase of rpm, viscosity increases for all the solutions. When rpm of the spindle is increased from 20 to 100, viscosity for EBB buffer, 3% PEG suspended in EBB buffer, 5% PEG suspended in EBB buffer and 10 % PEG suspended in EBB buffer increased from 2 cp to 12 cp, 4 cp to 17.6 cp, 8 cp to 18.4 cp and 10 cp to 24.4 cp, respectfully.

The non-Newtonian fluid does not obey newton's law of viscosity. Viscosity is independent of applied stress according to Newton's law. But for non-Newtonian fluid, viscosity depends on the applied stress. From Figure 11, the viscosity is changing with the increase of rpm. Because of this, it is safe to say that the fluid, used in our experiment, is a non-Newtonian fluid. For non-Newtonian fluid, viscosity is equal to shear stress divided by share rate.

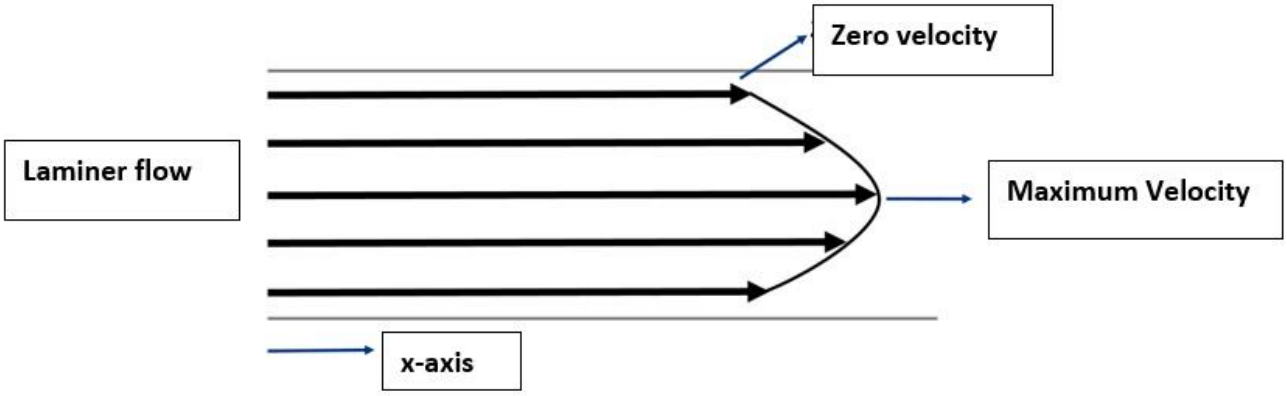


Figure 12: Velocity profile of laminar flow.

For laminar flow, at the boundary, velocity is zero and at the middle of the channel, the velocity is highest. So, the velocity gradually changes from zero to its maximum velocity. Velocity reaches Vmax in the middle of the height.

The flow channel had a rectangular cross-section of our experiment with a cross-section 1.85 mm x 0.12 mm.

In our experiment, for the first 100 -140 frames, no flow was present. As, the DNA is a flexible polymer and keeps fluctuating in the solution, to calculate the tethered point, the average position of the DNAs in this frame was considered as a tethered point of the DNA or unstarched DNA length.

Figure 13 shows the DNA stretching versus the time when DNA was stretched using 5% PEG in EBB buffer solution. The exposure rate of this experiment was 200 milliseconds. This means that data were taken every 200 milliseconds. From Figure 13, it is clear that for the first 20.6 seconds there is no flow, which means during the first 103 frames. Buffer flow starts after 103 frames. It takes few seconds to stretch the DNA fully. In figure 13, the DNA is fully stretched at around 38.2 seconds or 191 frames. From figure 13, DNA stretching divides into two parts: the first part is DNA stretching with EBB buffer and the second part is DNA stretching with 5% PEG in EBB buffer. DNA stretching for EBB buffer was sustained from 38 (or 190 frames) seconds to 85 seconds (or 450 frames). DNA stretching for 5% PEG in EBB buffer solution was sustained from 92 seconds (or 460 frames) to 400 seconds or (2000 frames). From this figure stretched length and fluctuation of DNA were calculated. The average position can be calculated from the average value for different conditions (See Fig 13). From the average position, the Stretched length of DNA can be calculated. Fluctuation of DNAs can be calculated from the standard deviation of the position of the Qdots (Fig. 13).

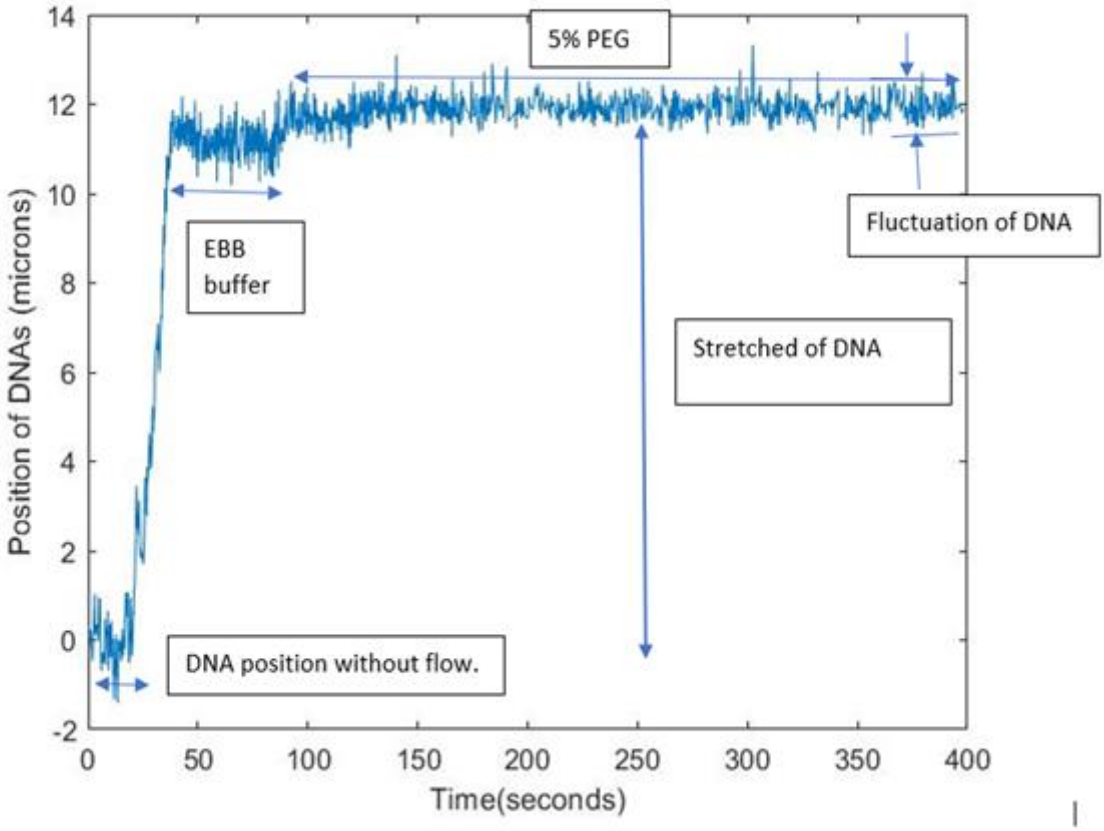


Figure 13: The stretched DNA length versus time.

Figure 14 shows the histogram for stretched DNA length and fluctuations of DNA for EBB buffer and the one with 3% PEG, respectively. In our experiment, the EBB buffer flowed with a 50 µl/min flowrate followed by a 3% PEG buffer.

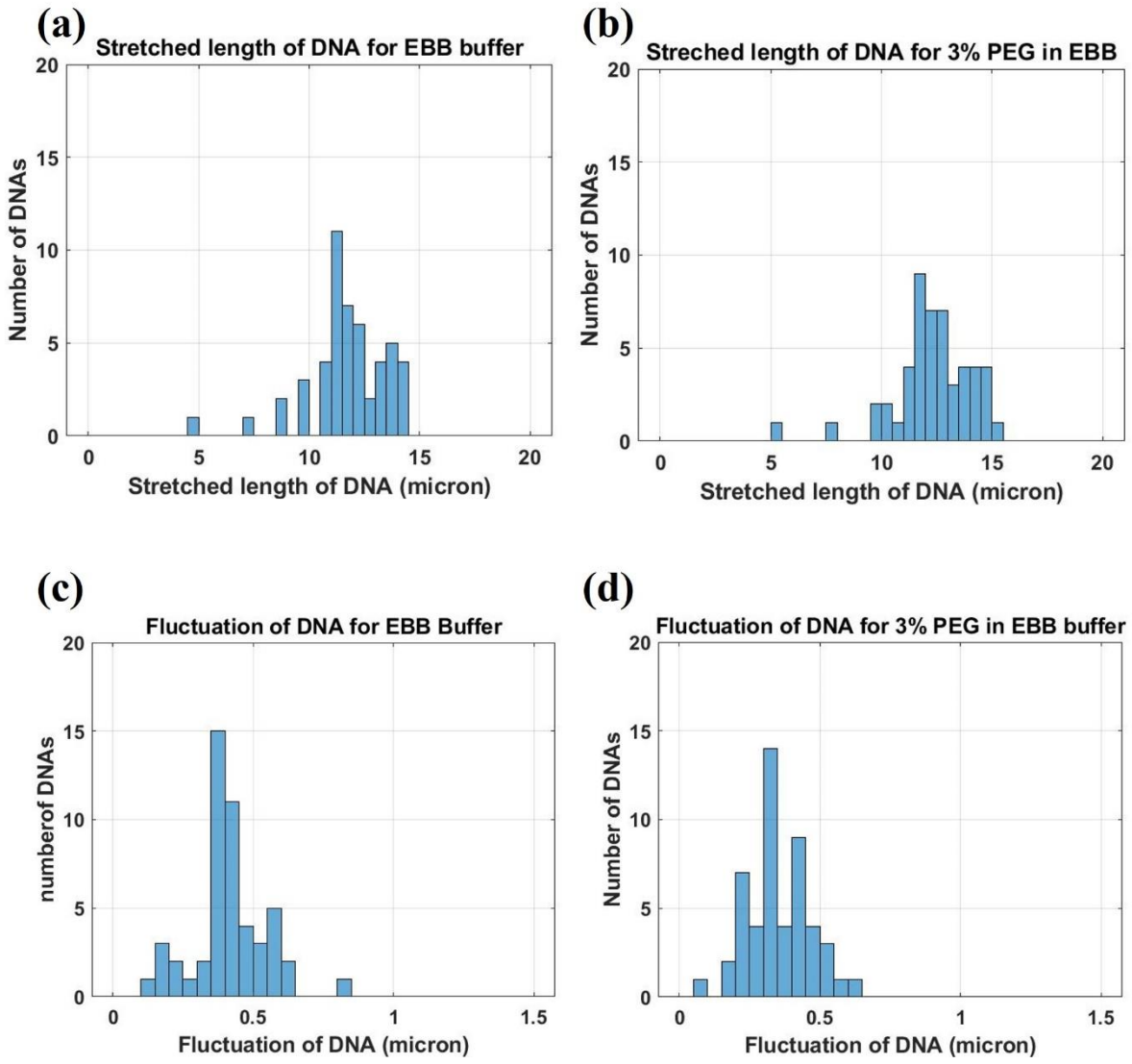


Figure 14: Histogram of flow-stretched DNA length and fluctuation of DNAs. a) Histogram of the flow-stretched length of DNA for EBB Buffer b) Histogram of the flow-stretched length of DNA for EBB Buffer containing 3% PEG c) Histogram of Fluctuation of DNA for EBB Buffer d) Histogram of Fluctuation of DNA for 3% PEG Buffer. The sample number is 50 from 2 different experiments.

In the above histogram, 50 samples were taken from 2 different experiments. From the above histogram, for stretching DNA with EBB buffer, the length between 11 µm to 11.5 µm has the highest frequency and length between 4.5 µm to 5 µm and 7 µm to 7.5 µm has the lowest frequency which is 1. For stretching DNA with 3% PEG suspended in EBB buffer, the length between 11.5 µm to 12 µm has the highest frequency and length between 5 µm to 5.5 µm and 7.5 µm to 8 µm has the lowest frequency which is 1. So, from this histogram, it can be observed that stretched length for DNAs has increased by 3% PEG suspended in EBB buffer. From these 50 samples, the average fluctuations for EBB buffer and 3% PEG in EBB buffer were 0.4168 µm and 0.3508 µm, respectively. So, the viscosity decreases by more than 15% when 3% PEG suspended in the EBB buffer solution was introduced in the flow channel.

Figure 15 shows a histogram for EBB buffer and 5% PEG. In this experiment, the EBB buffer has flowed at a 50 µl/min flow rate followed by a 5% PEG buffer.

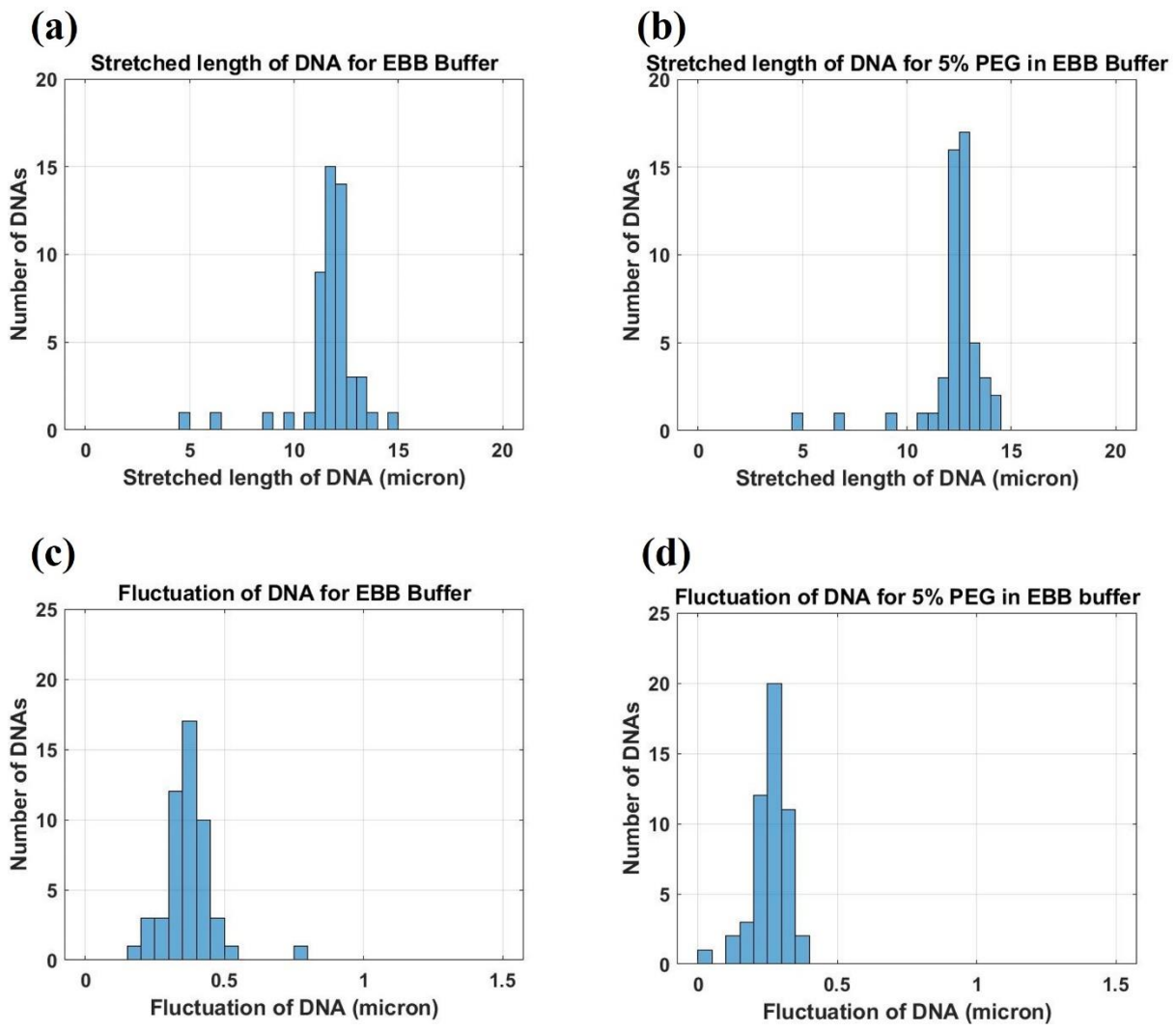


Figure 15: Histogram of stretched length and fluctuation of DNAs for 5% PEG solution in EBB buffer. a) Histogram of the stretched length of DNA for EBB Buffer b) Histogram of the stretched length of DNA for 5% PEG containing EBB buffer c) Histogram of Fluctuation of DNA for EBB Buffer d) Histogram of Fluctuation of DNA for 5% PEG Buffer. The Sample number is 51 which was taken from 3 different experiments.

In the above histogram, 51 samples were taken from 3 different experiments. From figure 15, it can be observed that for stretching DNA with EBB buffer, the length between 11.5 µm to 12 µm has the highest frequency and the length between 4.5 µm to 5 µm, 6 µm to 6.5 µm, 8.5 µm to 9 µm, 9.5 µm to 10 µm and 10.5 µm to 11 µm has the lowest frequency which is 1. For stretching DNA with 5% PEG in EBB buffer, the length between 12.5 µm to13 µm has the highest frequency and the length between 4.5 µm to 5 µm, 6.5 µm to7 µm, 9 µm to 9.5 µm, 10.5 µm to11 µm and 11 µm to 11.5 µm has the lowest frequency which is 1. Therefore, from this histogram, it can be stated that stretched length for DNAs has increased by 5 % PEG. The average fluctuations from the above 51 points for 5% PEG solution in EBB buffer were 0.2624 µm which was more than 28% lower than the fluctuation while using EBB buffer alone. The average fluctuation of DNAs for 3% PEG and 5% PEG are 15% and 28% lower than the fluctuations of DNAs for EBB buffer respectively. Thus, it can be concluded that DNA length and fluctuation are a function of viscosity.

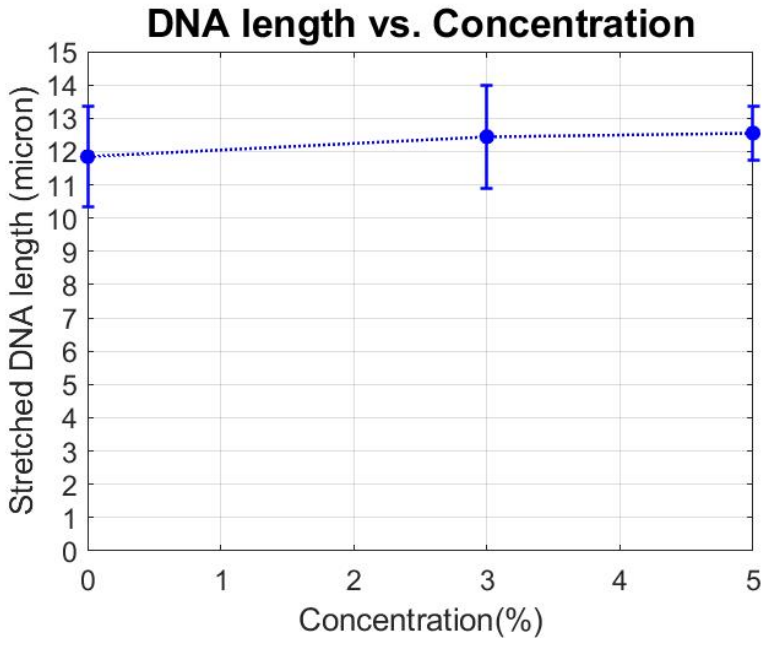


Figure 16: Flow-stretched length of DNA with PEG concentration in EBB buffer.

The above graph indicates that average length for 0% EBB is lower than 12 μm while the one for 5% EBB is ~12.5 μm. It implies only a 0.7 μm- 0.8 μm increase in length.

One of the reasons for the length extension upon using high viscosity fluid was the drag force. The drag force is directly proportional to velocity when the flow has a low Reynolds number. When a particle with a radius of r, moves with a velocity v in a fluid with viscosity η we can write:

$$F_d = 6\pi \eta v r$$

The length of DNA used in this experiment is 16 μm and the fluorescence-labeled quantum is 20 nm. DNAs are semi-flexible polymers. Therefore, the stretching of DNA depends on the applied force. The more the applied force is, the more the DNA will stretch out.

One of the reasons behind the decrease of fluctuation with increasing viscosity could be the compactness caused by the crowded environment. From the change of fluctuation, we can say that a crowded environment indeed influences the activity of biomolecules.

### 3.2 Effect of temperature on flow stretched DNA

As it has been stated above, temperature affects DNA twisting, overstretching transition of DNA, and DNA melting. Moreover, it was observed that if a thermal gradient is applied to DNA, it will cause some internal tension which will result in DNA stretching. In our experiment, the temperature gradient was not applied to the DNA; rather temperature was increased uniformly in all parts of the microfluidic flow cell. In our experiment, the stretching of DNA under various temperatures was investigated.

Figure 17 shows DNA stretching at different temperatures. Figure 17 can be divided into 7 regions; without any flow (o second to 47 seconds), 4 °C (63 seconds to 132 seconds), 10 ºC(336 seconds to 385 seconds), 15ºC (644 seconds to 690 seconds), 20ºC (945 seconds to 990 seconds), 25ºC (1168 seconds to 1190 seconds), and 30ºC (1432 seconds to 1460 seconds). From figure 17, a slight change in the DNA stretched length from temperature 4ºC to 30ºC was observed. Nevertheless, the change in fluctuation is difficult to tell just by looking at the figure. To calculate the fluctuation of the DNAs at the different temperatures, the standard deviation of length was calculated. Because of that, the unit of the fluctuations of the DNA was micron in this experiment.

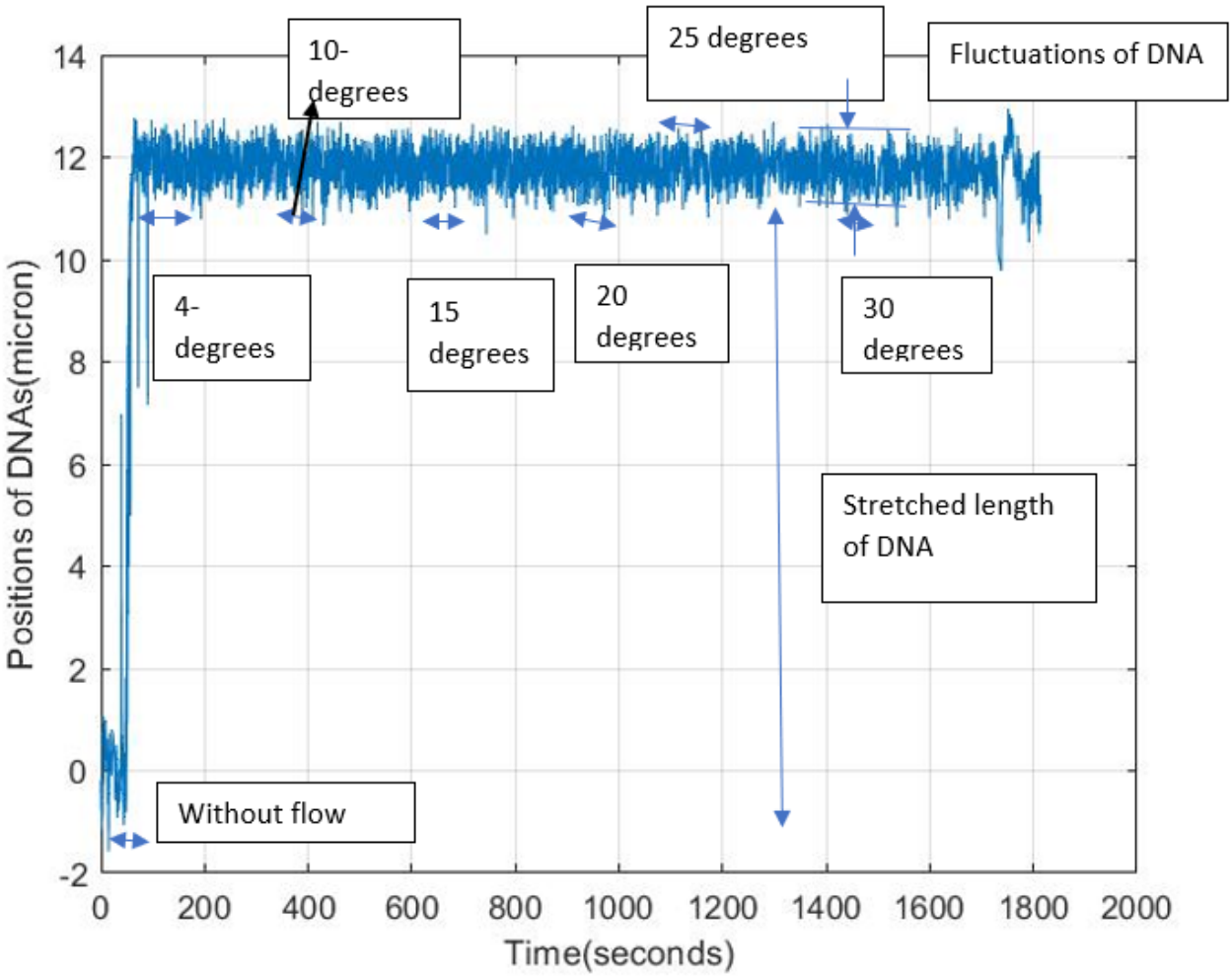


Figure 17: Stretching length of DNA versus time.

Figure 18 shows histograms for the length of DNA stretching at various temperatures. In this histogram, there are 50 data points are taking from 4 different experiments. The average stretched lengths of DNA for 4ºC, 10ºC, 15ºC, 20ºC, 25ºC, and 30ºC are 11.0360 ±1.2627 µm, 11.0706±1.3512 µm, 11.1914±1.2592 µm, 11.2708±1.2871 µm, 11.1890±1.2932 µm, and 11.4081±1.5542 µm respectively. There is a slight change in the average stretched length of DNA from 4ºC to 30ºC which is about 0.5 microns.

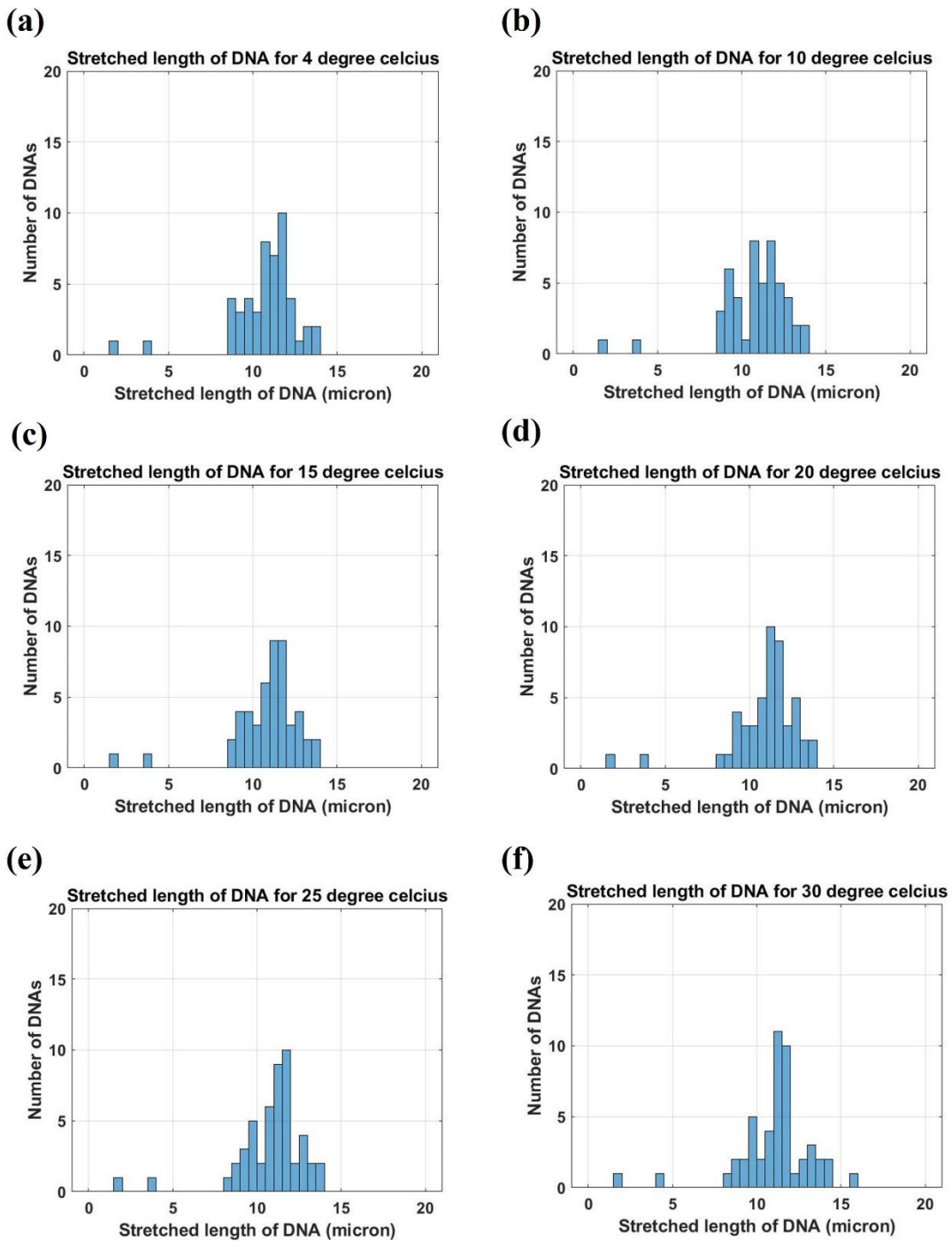


Figure 18: Histogram of the stretched length of DNAs for a) 4°C, b) 10 ºC, c)15 ºC, d) 20ºC, e) 25 °C, and) 30 ºC. The sample number is 50 which were taken from 4 different experiments.

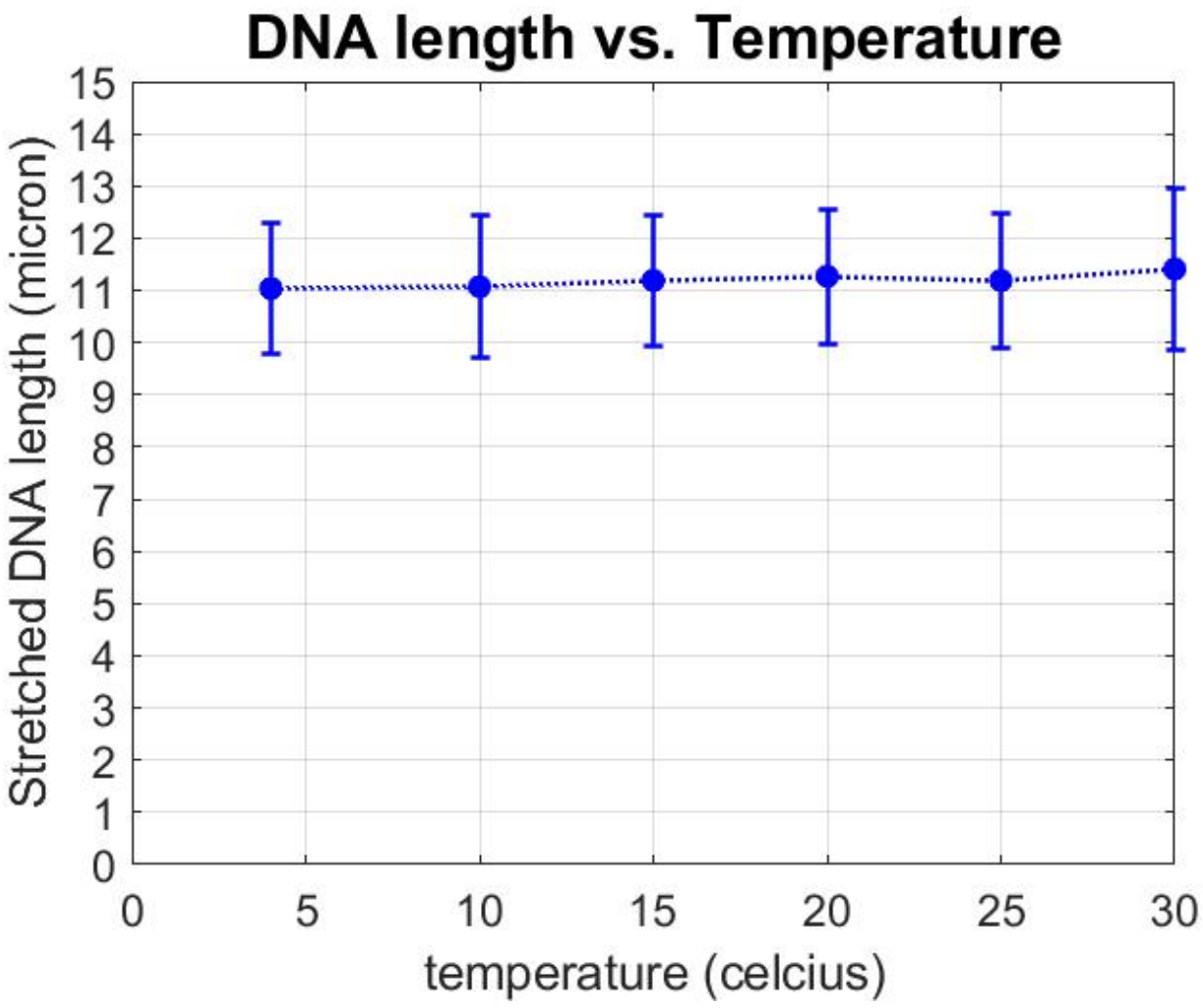


Figure 19: Stretched length of DNA versus Temperature.

From Figure 19 it can be observed that the average stretched-length of DNA increases from 4 ºC to 20 °C which is almost linear. Then the average stretched length of DNA decreases at a temperature of 25°C, and then increases again at a temperature of 30°C. Overall, the length change from 4°C to 30 °C is about 0.5µm. Jiang, H. R., & Sano, M. have found that if the temperature gradient is applied to DNA, they create internal tension on the DNA, and DNA stretches out. [36]. They measured conformations of one end tethered and two ends tethered DNA in different temperature gradients up to 3K⁄µm. They have observed that the length of

DNA increases with the increase of temperature gradient. Also, it was found that overstretching force depends on temperature. With the increase of temperature, overstretching force decreases. From our experiment, it was found out that temperature does influence the stretched length of DNA. So, it can be said that high temperature creates some pressure which in turn increases the stretching length of DNAs.

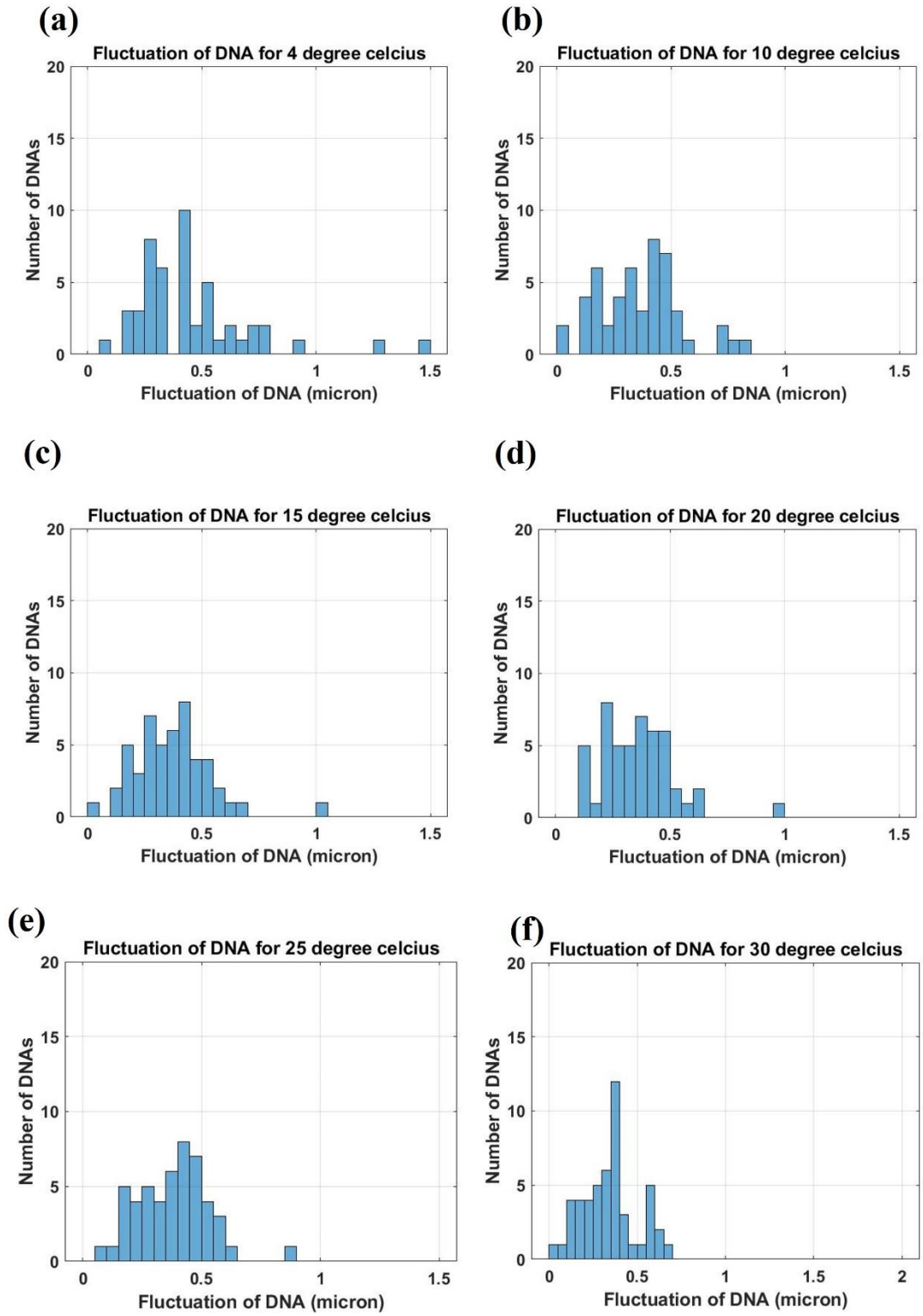


Figure 20: Histogram of fluctuation of DNAs for a) 4 ºC, b)10 °C c)15 ºC, d)20 °C, e) 25 °C, and e) 30 °C. The sample number is 50 which were taken from 4 different experiments.

Figure 20 shows the distribution of fluctuation of DNAs for different temperatures. There are 50 sample points from 4 different experiments. Average values of fluctuation for 4 ºC, 10 ºC, 15 ºC, 20 ºC, 25 ºC, and 30 ˚C are 0.4919 μm, 0.3638 μm, 0.3735 μm, 0.4302 μm, 0.3762 μm and 0.4163 μm, respectively. There is no definite trend in fluctuation with different temperatures. Temperature changes play little or no role in flow-stretched DNAs under our experimental conditions.

The data obtained from a series of single-molecule flow-stretching experiments with different temperatures and buffer viscosity indicate that the degrees of DNA stretching by flow (the length of flow-stretched DNAs) are affected by both temperature and viscosity. We also found out that buffer viscosities lead to changes in DNA fluctuations under flow. However, no noticeable changes in fluctuation were observed with different temperatures.

# CHAPTER IV

# CONCLUSION

In this experiment, single-molecule biophysics was used to study the effect of temperature and viscosity on flow-stretched DNA. From our experiment, it was found that temperature affects DNA stretching when the applied force is much lower than the overstretching force. The total increase of length from 4 °C to 30 °C was almost 0.5 μm which is almost linear. However, no noticeable change in the fluctuation of DNAs was observed with different temperatures. In future work, the effect of temperature on the fluctuation of the overstretching DNA will be studied.

Again, for viscosity, a significant change in the stretched length of DNA was found from our experiment. Also, the viscosity affects fluctuation. We saw a noticeable decrease in the fluctuation with the increase of viscosity. The average fluctuation for EBB buffer and 3% PEG in EBB buffer solution were 0.4168 μm and 0.3508 μm respectively. So, the DNA fluctuation decreases by more than 15%. The average fluctuations with 5% PEG solution in EBB buffer were 0.2624 micron which was more than 28% lower than the fluctuation while using EBB buffer. From this, it is clear that with the increase of the viscosity of buffer solution at a constant temperature, the Fluctuations of DNAs decreased. One of the reasons can be the compact environment created by high viscosity. Because of this compacted environment, high viscosity fluid can stretch DNA more than the lower viscosity fluid.

The total change of the stretched length of DNAs was changed almost 0.7 µm - 0.8 µm for 0 % PEG in EBB buffer to 5% PEG in EBB buffer solution in our experiment.

The experiment with 10 % PEG solution in EBB buffer was failed. it affects the surface passivation and DNA got stuck on the cover glass. In the future, 10 % PEG in buffer solution with better surface passivation can be used to do this experiment.

REFERENCES


[1] *McGraw-Hill encyclopedia of science & technology.*, 8th ed. New York: McGraw-Hill, 1997.

[2] H. B. Sun, J. Shen, and H. Yokota, "Size-Dependent Positioning of Human Chromosomes in Interphase Nuclei," *Biophys. J.*, vol. 79, no. 1, pp. 184–190, Jul. 2000, doi: 10.1016/S0006-3495(00)76282-5.

[3] H. Kim and J. J. Loparo, "Multistep assembly of DNA condensation clusters by SMC," *Nat. Commun.*, vol. 7, no. 1, p. 10200, Jan. 2016, doi: 10.1038/ncomms10200.

[4] A. Estévez-Torres and D. Baigl, "DNA compaction: fundamentals and applications," *Soft Matter*, vol. 7, no. 15, pp. 6746–6756, Jul. 2011, doi: 10.1039/C1SM05373F.

[5] I. Baeza *et al.*, "Electron microscopy and biochemical properties of polyamine-compacted DNA," *Biochemistry*, vol. 26, no. 20, pp. 6387–6392, Oct. 1987, doi: 10.1021/bi00394a012.

[6] K. Tsumoto, F. Luckel, and K. Yoshikawa, "Giant DNA molecules exhibit on/off switching of transcriptional activity through conformational transition," *Biophys. Chem.*, vol. 106, no. 1, pp. 23–29, Oct. 2003, doi: 10.1016/S0301-4622(03)00138-8.

[7] A. Houlton, A. R. Pike, M. A. Galindo, and B. R. Horrocks, "DNA-based routes to semiconducting nanomaterials," *Chem. Commun.*, no. 14, pp. 1797–1806, Apr. 2009, doi: 10.1039/B818456A.

[8] C. Wong, J. C. Santiago, L. Rodriguez-Paez, M. Ibánez, I. Baeza, and J. Oró, "Synthesis of putrescine under possible primitive earth conditions," *Orig. Life Evol. Biosph.*, vol. 21, no. 3, pp. 145–156, May 1991, doi: 10.1007/BF01809443.

[9] A. Mizuno and S. Katsura, "Manipulation of a Large DNA Molecule using the Phase Transition," *J. Biol. Phys.*, vol. 28, no. 4, pp. 587–603, Dec. 2002, doi: 10.1023/A:1021274319649.

[10] A. Ongaro *et al.*, "DNA-Templated Assembly of Conducting Gold Nanowires between Gold Electrodes on a Silicon Oxide Substrate," *Chem. Mater.*, vol. 17, no. 8, pp. 1959–1964, Apr. 2005, doi: 10.1021/cm047970w.

[11] A. Ongaro, F. Griffin, L. Nagle, D. Iacopino, R. Eritja, and D. Fitzmaurice, "DNA-Templated Assembly of a Protein-Functionalized Nanogap Electrode," *Adv. Mater.*, vol. 16, no. 20, pp. 1799–1803, 2004, doi: 10.1002/adma.200400244.

[12] E. Braun, Y. Eichen, U. Sivan, and G. Ben-Yoseph, "DNA-templated assembly and electrode attachment of a conducting silver wire," *Nature*, vol. 391, no. 6669, pp. 775–778, Feb. 1998, doi: 10.1038/35826.

[13] E. S. G. Shaqfeh, "The dynamics of single-molecule DNA in flow," *J. Non-Newton. Fluid Mech.*, vol. 130, no. 1, pp. 1–28, Oct. 2005, doi: 10.1016/j.jnnfm.2005.05.011.

[14] L. R. Brewer and P. R. Bianco, "Laminar flow cells for single-molecule studies of DNA-protein interactions," *Nat. Methods*, vol. 5, no. 6, pp. 517–525, Jun. 2008, doi: 10.1038/nmeth.1217.

[15] L. Y. Yeo, H.-C. Chang, P. P. Y. Chan, and J. R. Friend, "Microfluidic Devices for Bioapplications," *Small*, vol. 7, no. 1, pp. 12–48, 2011, doi: 10.1002/smll.201000946.

[16] D. B. Weibel and G. M. Whitesides, "Applications of microfluidics in chemical biology," *Curr. Opin. Chem. Biol.*, vol. 10, no. 6, pp. 584–591, Dec. 2006, doi: 10.1016/j.cbpa.2006.10.016.

[17] M. Spies, P. R. Bianco, M. S. Dillingham, N. Handa, R. J. Baskin, and S. C. Kowalczykowski, "A Molecular Throttle: The Recombination Hotspot χ Controls DNA Translocation by the RecBCD Helicase," *Cell*, vol. 114, no. 5, pp. 647–654, Sep. 2003, doi: 10.1016/S0092-8674(03)00681-0.

[18] P. Grayson, L. Han, T. Winther, and R. Phillips, "Real-time observations of single bacteriophage λ DNA ejections in vitro," *Proc. Natl. Acad. Sci.*, vol. 104, no. 37, pp. 14652–14657, Sep. 2007, doi: 10.1073/pnas.0703274104.

[19] P. R. Bianco, J. J. Bradfield, L. R. Castanza, and A. N. Donnelly, "Rad54 Oligomers Translocate and Cross-bridge Double-stranded DNA to Stimulate Synapsis," *J. Mol. Biol.*, vol. 374, no. 3, pp. 618–640, Nov. 2007, doi: 10.1016/j.jmb.2007.09.052.

[20] C. Bustamante, "Unfolding single RNA molecules: bridging the gap between equilibrium and non-equilibrium statistical thermodynamics," *Q. Rev. Biophys.*, vol. 38, no. 4, pp. 291–301, Nov. 2005, doi: 10.1017/S0033583506004239.

[21] P. R. Selvin and T. Ha, *Single-molecule techniques*. Cold Spring Harbor Laboratory Press, 2008. Accessed: Jul. 19, 2021. [Online]. Available: https://agris.fao.org/agris-search/search.do?recordID=US201300125747

[22] A. A. Deniz, S. Mukhopadhyay, and E. A. Lemke, "Single-molecule biophysics: at the interface of biology, physics and chemistry," *J. R. Soc. Interface*, vol. 5, no. 18, pp. 15–45, Jan. 2007, doi: 10.1098/RSIF.2007.1021.

[23] X. Michalet, S. Weiss, and M. Jäger, "Single-Molecule Fluorescence Studies of Protein Folding and Conformational Dynamics," *Chem. Rev.*, vol. 106, no. 5, pp. 1785–1813, May 2006, doi: 10.1021/cr0404343.

[24] X. Nan, P. A. Sims, P. Chen, and X. S. Xie, "Observation of Individual Microtubule Motor Steps in Living Cells with Endocytosed Quantum Dots," *J. Phys. Chem. B*, vol. 109, no. 51, pp. 24220–24224, Dec. 2005, doi: 10.1021/jp056360w.

[25] P. Guptasarma, "Does replication-induced transcription regulate synthesis of the myriad low copy number proteins of Escherichia coli?," *BioEssays*, vol. 17, no. 11, pp. 987–997, 1995, doi: 10.1002/bies.950171112.

[26] S. Ghaemmaghami *et al.*, "Global analysis of protein expression in yeast," *Nature*, vol. 425, no. 6959, pp. 737–741, Oct. 2003, doi: 10.1038/nature02046.

[27] G. Binnig and H. Rohrer, "Scanning tunneling microscopy," *Surf. Sci.*, vol. 126, no. 1, pp. 236–244, Mar. 1983, doi: 10.1016/0039-6028(83)90716-1.

[28] F. J. Giessibl, "Advances in atomic force microscopy," *Rev. Mod. Phys.*, vol. 75, no. 3, pp. 949–983, Jul. 2003, doi: 10.1103/RevModPhys.75.949.

[29] G. V. Shivashankar, M. Feingold, O. Krichevsky, and A. Libchaber, "RecA polymerization on double-stranded DNA by using single-molecule manipulation: The role of ATP hydrolysis," *Proc. Natl. Acad. Sci.*, vol. 96, no. 14, pp. 7916–7921, Jul. 1999, doi: 10.1073/pnas.96.14.7916.

[30] P. Cluzel *et al.*, "DNA: An Extensible Molecule," *Science*, vol. 271, no. 5250, pp. 792–794, Feb. 1996, doi: 10.1126/science.271.5250.792.

[31] T. Funatsu, Y. Harada, M. Tokunaga, K. Saito, and T. Yanagida, "Imaging of single fluorescent molecules and individual ATP turnovers by single myosin molecules in

aqueous solution," *Nature*, vol. 374, no. 6522, pp. 555–559, Apr. 1995, doi: 10.1038/374555a0.

[32] A. Yildiz, J. N. Forkey, S. A. McKinney, T. Ha, Y. E. Goldman, and P. R. Selvin, "Myosin V Walks Hand-Over-Hand: Single Fluorophore Imaging with 1.5-nm Localization," *Science*, vol. 300, no. 5628, pp. 2061–2065, Jun. 2003, doi: 10.1126/science.1084398.

[33] H. Kim and P. R. Selvin, "Fluorescence Imaging with One Nanometer Accuracy," Encycl. Biophys., pp. 803–809, 2013, doi: 10.1007/978-3-642-16712-6_511.

[34] N. Ostrowska, M. Feig, and J. Trylska, "Modeling Crowded Environment in Molecular Simulations," *Front. Mol. Biosci.*, vol. 0, 2019, doi: 10.3389/fmolb.2019.00086.

[35] M. C. Williams, J. R. Wenner, I. Rouzina, and V. A. Bloomfield, "Entropy and Heat Capacity of DNA Melting from Temperature Dependence of Single-Molecule Stretching," *Biophys. J.*, vol. 80, no. 4, pp. 1932–1939, Apr. 2001, doi: 10.1016/S0006-3495(01)76163-2.

[36] R. E. Thompson, D. R. Larson, and W. W. Webb, "Precise Nanometer Localization Analysis for Individual Fluorescent Probes," *Biophys. J.*, vol. 82, no. 5, pp. 2775–2783, May 2002, doi: 10.1016/S0006-3495(02)75618-X.

[37] "Fluid Biomechanics," in *Sport and Exercise Science*, 2nd ed., Routledge, 2012.

[38] A. M. Abdullah *et al.*, "Tailoring the viscosity of water and ethylene glycol based TiO2 nanofluids," *J. Mol. Liq.*, vol. 297, p. 111982, Jan. 2020, doi: 10.1016/j.molliq.2019.111982.

[39] F. Kriegel *et al.*, "The temperature dependence of the helical twist of DNA," *Nucleic Acids Res.*, vol. 46, no. 15, pp. 7998–8009, Sep. 2018, doi: 10.1093/nar/gky599.

[40] H.-R. Jiang and M. Sano, "Stretching single molecular DNA by temperature gradient," *Appl. Phys. Lett.*, vol. 91, no. 15, p. 154104, Oct. 2007, doi: 10.1063/1.2775810.

[41] J. F. Marko and E. D. Siggia, "Bending and Twisting Elasticity of DNA Volume 27, Number 4, February 14, 1994, pp 981−988," *Macromolecules*, vol. 29, no. 13, pp. 4820–4820, Jan. 1996, doi: 10.1021/ma9520104.

[42] C. Bouchiat, M. D. Wang, J.-F. Allemand, T. Strick, S. M. Block, and V. Croquette, "Estimating the Persistence Length of a Worm-Like Chain Molecule from Force-

Extension Measurements," *Biophys. J.*, vol. 76, no. 1, pp. 409–413, Jan. 1999, doi: 10.1016/S0006-3495(99)77207-3.

[43] H. Fu, H. Chen, J. F. Marko, and J. Yan, "Two distinct overstretched DNA states," *Nucleic Acids Res.*, vol. 38, no. 16, pp. 5594–5600, Sep. 2010, doi: 10.1093/nar/gkq309.

[44] A. E. Cohen and W. E. Moerner, "Principal-components analysis of shape fluctuations of single DNA molecules," *Proc. Natl. Acad. Sci.*, vol. 104, no. 31, pp. 12622–12627, Jul. 2007, doi: 10.1073/pnas.0610396104.

[45] Axelrod, Daniel. "Total internal reflection fluorescence microscopy in cell biology." Traffic 2, no. 11 (2001): 764-7

[46] Reck-Peterson, Samara L., Nathan D. Derr, and Nico Stuurman. "Imaging single molecules using total internal reflection fluorescence microscopy (TIRFM)." Cold Spring Harbor Protocols 2010, no. 3 (2010): pdb-top73.

[47] Gore, Jeff, Zev Bryant, Marcelo Nöllmann, Mai U. Le, Nicholas R. Cozzarelli, and Carlos Bustamante. "DNA overwinds when stretched." Nature 442, no. 7104 (2006): 836-839.

[48] Kim, HyeongJun, and Joseph J. Loparo. "Observing bacterial chromatin protein-DNA interactions by combining DNA flow-stretching with single-molecule imaging." In Bacterial Chromatin, pp. 277-299. Humana Press, New York, NY, 2018.

# BIOGRAPHICAL SKETCH

Fatema Tuz Zohra completed his BSc in Mechanical Engineering from the Bangladesh University of Engineering and technology in 2017. She joined the Department of Mechanical Engineering at the University of Texas Rio Grande Valley in 2019. She worked with Dr. HyeongJun Kim Dr. Horacio Vasquez for her master thesis. She also worked as Graduate Teaching Assistant under Dr. Horacio Vasquez. I have graduated on August, 2021 with my master's degree. My contact address is fatemabuet25@gmail.com.